Fatigue life prediction of centrifugal fan blades in the ventilation cooling system

of the high-speed-train

N. He [1], PF Feng [1], ZW Li [1], LG Tan [1, *], L. Mo[3], T. Pang [1], YZ Chen [2], C. Yang [2]

[1] State Key Laboratory of Advanced Design and Manufacture for Vehicle Body, Hunan University, Changsha, 410082, China

[2] Zhuzhou CRRC times electric co, LTD, Zhuzhou, 412001, China

[3] School of Food Sciences and Engineering, South China University of Technology, Guangzhou 510641, PR China

Abstract: The centrifugal fan blades of the high-speed train ventilation and cooling system are subjected to cyclic loading which will shorten the life of fan blades. It could cause an accident of the high-speed-train in service. In this study, a modified method based on the nominal stress method was proposed and developed for the fatigue life prediction of centrifugal fan blades. The finite element model was firstly used to analyze the mode and the stress of fan blades based on the typical material property. The fatigue life was predicted based on the physical curve, using the Miner's cumulative damage rule to calculate total damage. In order to verify the effectiveness of this method, the experimental tests were conducted on fan blades using a fatigue bench system, which were the typical structure of the ventilation cooling system of the high-speed-train. The damage mechanisms of blades was deduced from the fracture fractographs. The ventilation good correlation was achieved between the prediction model and the actual experimental results, testifying the practicability and effectiveness of this proposed method. Thus, the research result can reduce the probability of

State Key Laboratory of Advanced Design and Manufacture for Vehicle Body, * Corresponding author. State Key Laboratory of Advanced Design and Manufacturing for Vehicle Body, Hunan University, Changsha 410082, China.
  Email address: tlg9@163.com (Ligang Tan).

accidents caused by the fan blade damage and improve the reliability of the ventilation cooling system of the high-speed train.

1. Introduction

The centrifugal fans are mainly used for the cooling of traction motors, main transformer cabinets and auxiliary transformer cabinets of the high-speed trains. As one of the main components of rail transportation equipment, the safety and reliability of the centrifugal fans deserves more attentions and studies. The centrifugal fans of the high-speed trains always operates in vibration conditions and the start-stop operation module would cause the change of the loads applied on the fans. The loads can be usually described by the deterministic formulas or stochastic theory [1]. On the other hand, the start-stop operation module would result in alternating stress in fan blades, which is the main reason for the fatigue failure. The high cycle fatigue life consumption [2], caused by alternating stress should be considered during the working process of the fans. Therefore, the assessment of fatigue life is necessary for the design of fan blades and an important index for evaluating their reliability. Additionally, it has important theoretical meanings and practical applications for the fatigue life assessment of the centrifugal fan blades.

The nominal stress method is the most traditional tool used to predict the fatigue life of a mechanical device. [3-5]. Some researchers conducted the fatigue analysis for compressor blades and the crack initiation and propagation in blades were simulated based on the static and dynamic stress analysis coupled with the development of fracture mechanics criteria [6, 7]. The finite element

method and the fluid and structure interaction method are always used to calculate the stress in the fan blades and is the key technique of understanding fatigue characteristics and failure mechanisms, and then the stress can be used to predict the fatigue life of the structure [8-10]. Abdullahi et al. [11] conducted a life assessment for the aero jet engine blades based on the finite element analysis and the Neu/Sehitoglu (N/S) TMF model. The finite element analysis coupled with the *S-N* method can be also used to assess the low cycle fatigue life of steam turbine blade [12], and to predict the catastrophic failure of turbine blade arisen from fatigue [13]. Due to the complex operating condition of fan blades, the low cycle fatigue (LCF) and the high cycle fatigue (HCF) may both contribute to the fatigue failure of the structural component, and the influence of interaction of the LCF and the HCF of fan blades under aerodynamic and static structural loads were also studied by some researches [14-16]. Considering all the static and dynamic loads applied on fans, the fatigue caused by the combined cycle loads was investigated by using the experimental method coupled with analytical methods [17-20]. Miner's rule is the mostly used cumulative damage models to evaluate the fatigue failures of a structure component, the fatigue life estimation of helicopter main rotor blade under random load [21], the fatigue life prediction for turbine blades , however, the coupling fatigue damage due to the effects of different loads interactions were ignored [22, 23]. For some blade components working in a high temperature environment, such as gas turbine blades, the thermo-mechanical fatigue effects should not be ignored and the fatigue life prediction should be conducted considering the mechanical and thermal analysis [24-26]. Meanwhile, The research on the dynamic characteristics of fan blades mainly focuses on gas turbine blades [27], compressor blades [28], steam turbines [29], wind turbine blades [30, 31], wings [32], helicopter blade [33] and there are few studies on fan blades in the ventilation and cooling system of railway locomotives. It's

critical to design the fan blades of many railway vehicles, but the fatigue design experiments of each type of fan structure are costly and time consuming. Therefore, a reliable fatigue life prediction model is essential for the design and optimization of the fan blades.

This paper aimed to develop a model for the fatigue life prediction of fan blades in the ventilation cooling system of the high-speed-train. Focusing on the causes of the dynamic stress of the fan blade, the fatigue life of a typical centrifugal fan blade was investigated. At first, the chemical composition analysis, static tensile test and dynamic fatigue test for the blade material of DC51D+Z were conducted. The basic composition and mechanical property parameters of the material were obtained from the experimental tests, and the *S-N* curve of the material DC51D+Z was fitted based on the experimental data. Considering the influence of friction and contact force of its structural parts, the stress distribution at the critical point of blade components was obtained by the finite element analysis. In the present study, considering the load patterns, size effects, surface morphology and stress concentration factor (SCF) of the fan blade comprehensively, an improved method based on the concept of the nominal stress is introduced. Finally, in order to prevent the fan blade from damaging caused by the fatigue under unexpected circumstances, a new model for predicting the fatigue life of fan blades in the ventilation cooling system of the high-speed-train is established. Combined the Palmgren-Miner cumulative damage criterion with the *S-N* curve, the fatigue life prediction model is established.

2. Material and properties

2.1. Material

Table 1

Chemical analysis of the fractured blades.

Elements	C	Si	Mn	P	S
Result of DC51D+Z	0.03	0.01	0.2	0.0015	0.0013

The chemical composition of the fractured blade was analyzed by emission spectrometry. The results were showed in Table 1. The results showed that the blade material was consistent with the analysis results of DC51D+Z steel, and it was a commonly steel used for centrifugal fan blades.

Based on ISO 6892-1:2009, MOD standard, the tensile test was carried out with MTS-809 test machine at room temperature at a loading speed of 1 mm/min. Dimensions of tensile test specimens were illustrated in Fig.1. The average yield stress(σ_s), ultimate strength$(\sigma_b)$and elastic modulus(E) of the three testing samples were listed in Table 2.
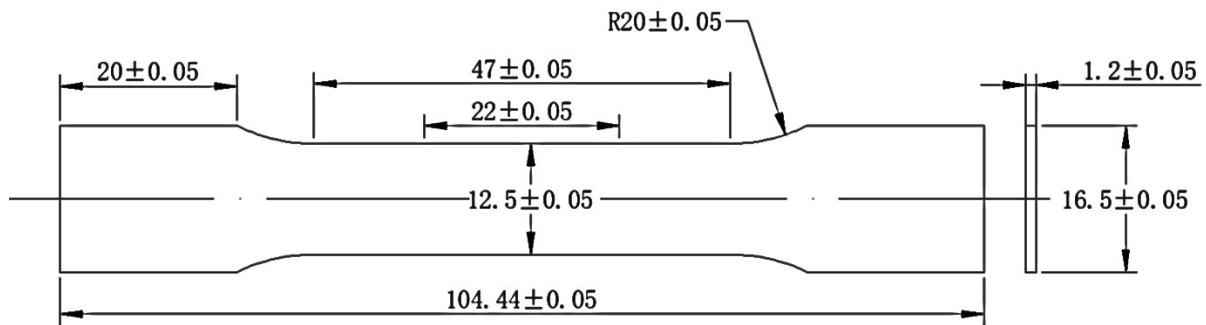
Fig.1. Dimensions (in mm) of tensile specimens.

Table 2

Tensile test results for the blade.

| Sample	Thickness(mm)	Width, mm	σ_s(MPa)	σ_b(MPa)	E(MPa)
DC51D+Z	1.2	12.5	290	364	206

2.2. Fatigue tests

Fatigue tests were conducted on a GPS-100 test machine at room temperature in air ambient based on ISO 1099:2006, MOD standard. The loading frequency was 126 Hz and the stress ratio is -1 ($R = \sigma_{min}/\sigma_{max}$). Four groups of the fatigue life tests were performed on the standard specimens at

four different stress amplitude levels, and at least five specimens were used for each group.

Before the start of the fatigue tests, to reduce the impact of surface defects on the fatigue life, 2000 mesh emery paper was used to polish the middle sections of the specimens to ensure that there was no obvious scratch existing on the polished areas. Fig. 2A and B showed the fatigue test specimens and the fatigue test process, respectively.
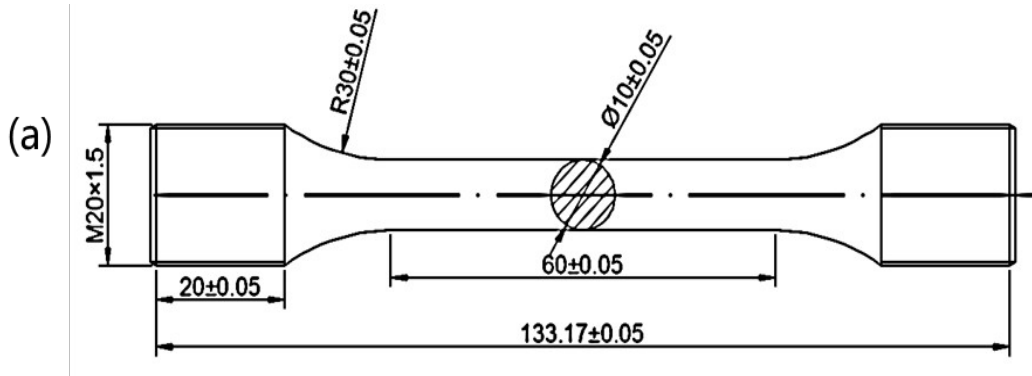
(A)
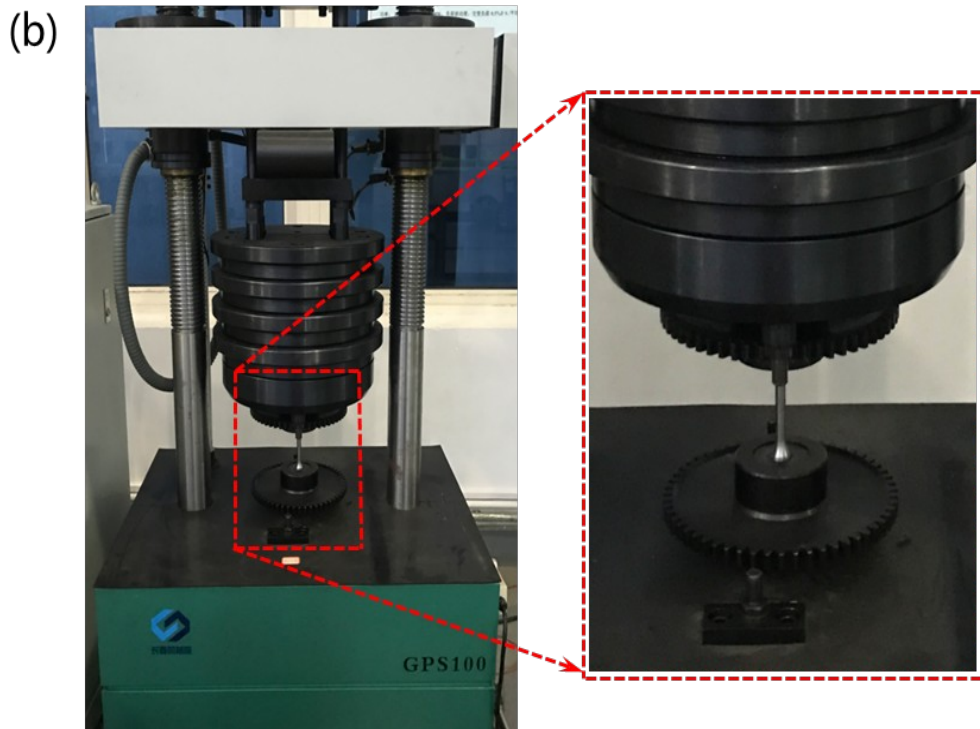
(B)

Fig.2. The material fatigue test. (A) Dimensions (in mm) of fatigue specimens.(B) Photograph of

fatigue test set-up.

The *S-N* curve which accurately reflected the fatigue properties of materials was a necessary prerequisite for the life estimation of structural components [34]. Some empirical models, such as two-parameter powers or exponents, were widely used. The fatigue curve for DC51D+Z material was a curve describing the relationship between its stress level and fatigue life, which was approximate to a straight line in logS-logN coordinates. Therefore, in this paper, the exponential function formula was selected to represent the DC51D+Z curve:

$$\log N = a + b \log \sigma \tag{1}$$

where σ represents the stress level of the test. N is the stress cycle number of fatigue failure. a and b are the material constants.

The fitting *S-N* curve of DC51D+Z based on the least square method was shown in Fig.3.
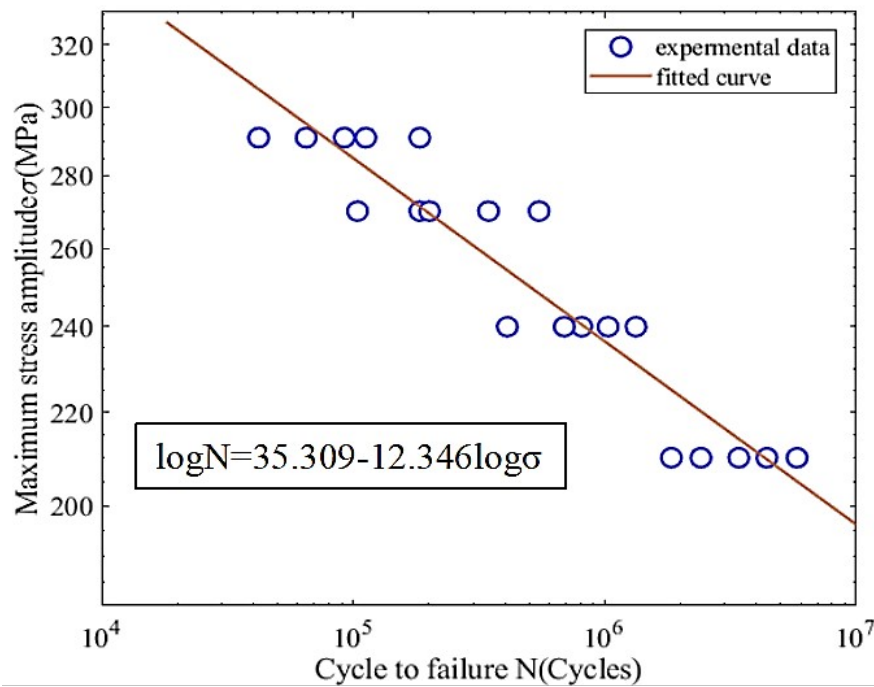

Fig.3. The *S-N* curve for DC51D+Z material.

As shown in Fig.3, the *S–N* curve of DC51D+Z at a stress ratio of -1 can be defined as:

7

$$\log N = 35.309 - 12.346 \log \sigma \qquad (2)$$

3. Fatigue life prediction

3.1. Finite element model

The experimental fan blade specimen was shown in Fig.4A. The fan was composed of hub, wheel and 60 blades. When the fan was driven by variable frequency motor to rotate, the blades were under the interactive fatigue load for a long time, which may lead to the blades fatigue failure under a certain number of cycles. The finite element model of the fan blade was established to simulate the working condition of the fan blade, so as to determine the dynamic stress distribution of the fan blade, the maximum stress in the stress concentration area and the possible failure position of the blade[35]. In this study, we used ANSYS software for analysis and a 3D finite element model of fan blade was established. Considering the complex geometric structure of the fans, the finite element model consisted of 427 K solid 185 element, which is a kind of 8 nodes solid hexahedron element. The mesh size was 0.4~5 mm, and 1.1 million hexahedron meshes were divided, as shown in Fig.4B Considering the influence of friction force and contact force of structural parts of fan, centrifugal force was applied by exerting an angular velocity on the finite element model.
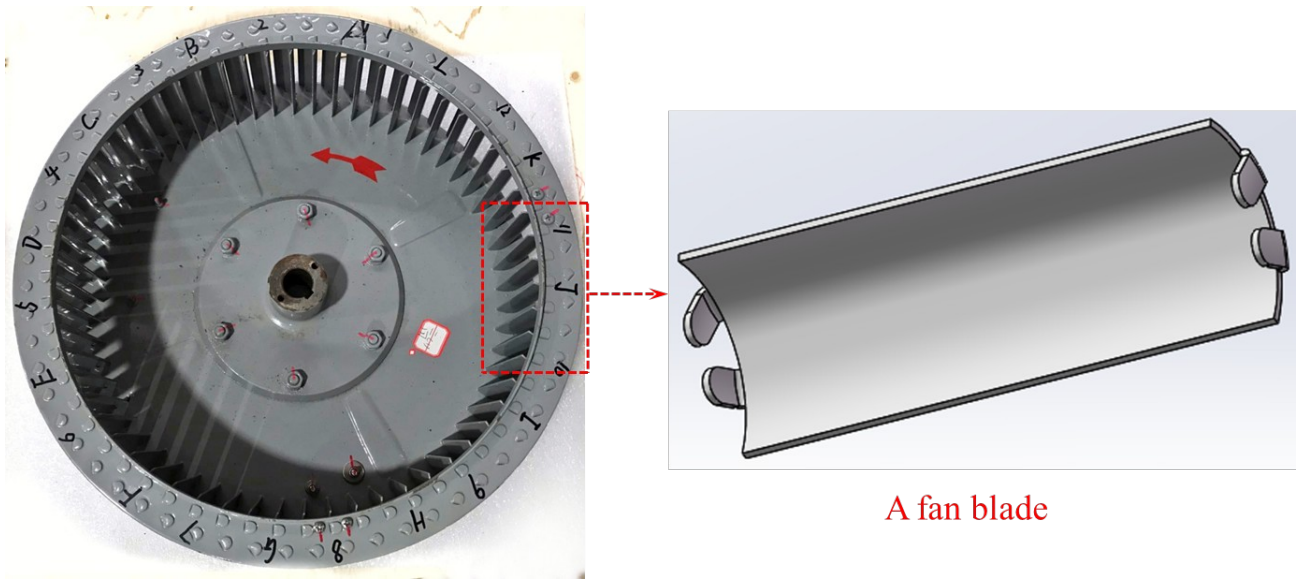
A fan blade

(A)
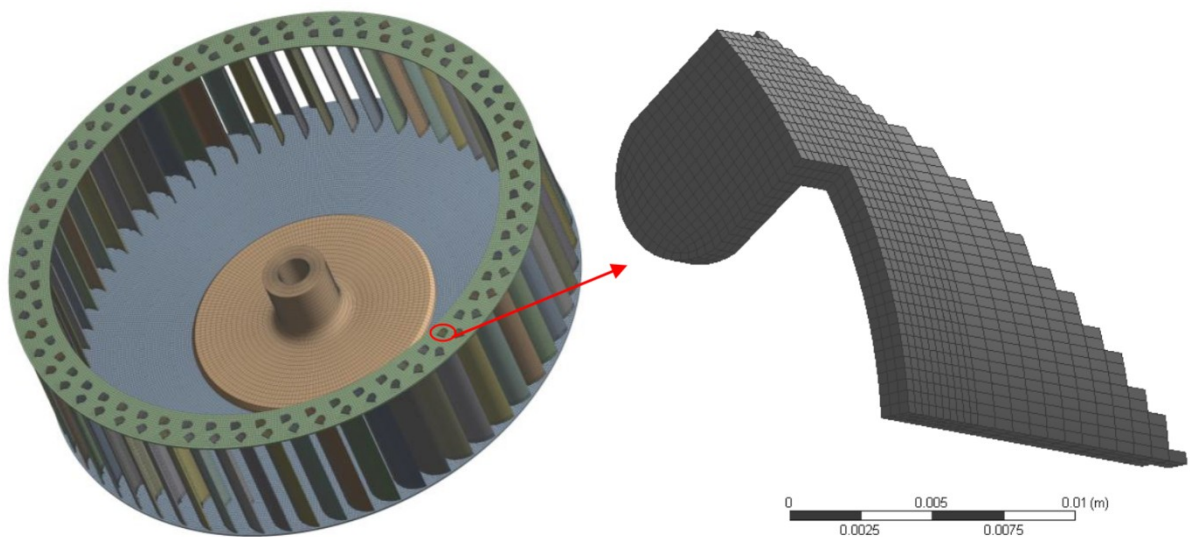
(B)

Fig.4. The fan blade. (A) Centrifugal fan blades for the fatigue tests. (B) Meshed model of the centrifugal fan blade.

3.2. Stress analysis

Modal analysis was carried out to examine the dynamic behavior of blades in service. The natural frequencies of the system and relevant mode shapes were calculated. The analysis showed

that the first natural frequency was 57.1 Hz; the other three frequencies are 57.4 Hz, 89.8 Hz and 285.5 Hz, respectively. The first natural frequency of the blade was higher than the blade's rotation frequency of 26.7 Hz (1600 rpm), so it would not cause resonance. The other three higher frequencies would not induce any resonance too.

Based on the finite element method, the stress distribution for the blades under the centrifugal load was computed. As shown in table 3, the maximum von Mises stress and the corresponding X-direction stress for the blades under revolving speeds of 1600, 1800 and 2000 rpm were obtained. The model was also used to conduct an approximate aerodynamic analysis for blades to estimate the stress in the blades caused by aerodynamic load. The maximum stress occurred in the root area of blades, as shown in Fig.5. According to the finite element analysis, the magnitude of stress caused by aerodynamic was 4.4 MPa.
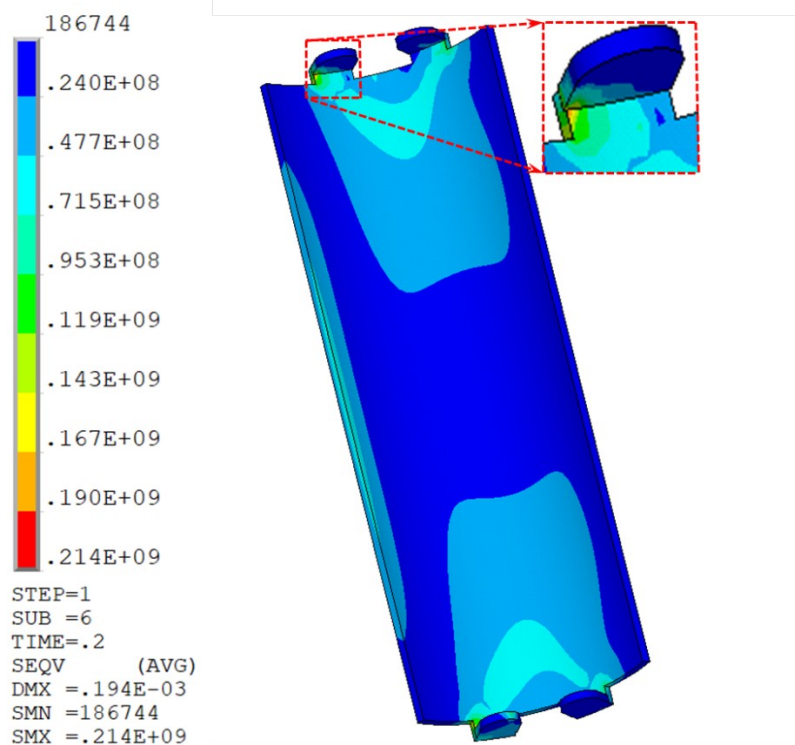
Fig.5. Dynamic stress distribution, arrow shows the location of maximum stress.

Table 3

Finite element analysis of the maximum stress of blade and X-direction stress.

Revolving speed(rpm)	Von Mises stress(MPa)	X-direction stress(MPa)
1600	214.12	56.04
1800	235.20	61.41
2000	258.30	67.43
2200	282.41	73.10

3.3. Prediction model for the fatigue life

In general, the fatigue properties of materials or structures are represented by the *S-N* curves. In this paper, the *S-N* curve of the fan structure is predicted by the material *S-N* curve combined with the nominal definition method [36].

$$S = \frac{\beta \varepsilon \, C_L}{K_T} \sigma \tag{3}$$

where *S* and σ represent the fatigue limit of structural components and material when the stress ratio *R* is -1 respectively. K_T is the stress concentration coefficient. ε is the size effect coefficient. β is the surface quality coefficient. C_L is loading method.

In order to obtain more accurate stress-life relationship of structural parts, the *S-N* curve of material parts should be modified. The stress concentration factor (SCF) had a great influence on the fatigue of structural components [37], which could be calculated according to the value of the maximum stress obtained from finite element model and the nominal stress value [38]. The stress concentration coefficient can be defined as

$$K_T = \frac{\sigma_{max}}{\sigma_0}$$ (4)

where σ_{max} is the maximum stress value at the stress concentration and σ_0 is the nominal stress value.

The nominal strength of a particular material varies with the size of the sample. The effect of size on the strength and fatigue properties of structural materials has been observed experimentally[39]. The size effect can be expressed as

$$\varepsilon = \frac{S_L}{S_S}$$ (5)

where S_L is the fatigue strength of large-size specimens and S_S is the fatigue strength of standard small size specimens.

Substituting Eqs. (4) and (5) into Eq. (3) results in

$$S = \frac{\beta \varepsilon S_L \sigma_0}{S_S \sigma_{max}} \sigma$$ (6)

It should be noted that the fatigue test was generally only carried out at the specific load ratio of R_0 to confirm the fatigue performance of similar structural details. In other words, the S-N curve was only applicable to describe the fatigue performance when a specific value was R_0. On the contrary, in the actual load history, there were a lot of different conditions of stress cycle stress ratio. Therefore, it was necessary to modify the S-N curve by using the empirical constant life diagram to make it applicable to the stress cycles with different stress ratios in the history of actual loads. Some empirical constant life charts, for example Goodman, modified Goodman (i.e., Smith or Soderberg), Bagci and Gerber charts were widely used. Nevertheless, by reanalyzing the charts above, it was known that [40] the modified Goodman(i.e., Smith or Soderberg) for most materials' fatigue limit

12

estimates were conservative. Bagci model was optimistic for majority of materials. Gerber equation was applied to ductile materials but its application was limited by its nonlinear function. Goodman chart was suitable for brittle materials, but being conservative for ductile materials. Therefore, the empirical Goodman chart [41, 42] was adopted to modify the *S-N* curve as:

$$\frac{S_a}{S_{-1}} + \frac{S_m}{\sigma_b} = 1 \tag{7}$$

where S_a is the nominal stress amplitude. S_m is the mean nominal stress. S_{-1} is the fatigue limit of structural components when the stress ratio R is -1 and σ_b is the tensile strength of the material.

Stress amplitude can be written as

$$S_a = \frac{S_{max} - S_{min}}{2} \tag{8}$$

where S_{max} and S_{min} are the maximum and minimum the nominal stress correspondingly.

Mean stress can be defined as

$$S_m = \frac{S_{max} + S_{min}}{2} \tag{9}$$

According to the definition of the stress ratio, it can be displayed that

$$R = \frac{S_{min}}{S_{max}} = \frac{S_m - S_a}{S_m + S_a} \tag{10}$$

Taking transformation of Eq.(8)gives, Goodman's graph shows the linearity when the specific load ratio is R_0:

$$\frac{S_{a,R_0}}{S_{-1}} + \frac{S_{m,R_0}}{\sigma_b} = 1 \tag{11}$$

where S_{a,R_0} and S_{m,R_0} are the nominal stress amplitude and the mean nominal stress when a load ratio

is R_0.

The equivalent life curve was obtained by using the Goodman curve, and based on the working stress of the fan provided by the supplier, the stress of the fan structure was modified [43]. The modified curve was shown in Fig. 6 and Eq. (12). The predicted life of four different rotating speeds was shown in Table 4.

$$\log N = 49.047 - 18.691 \log S \tag{12}$$
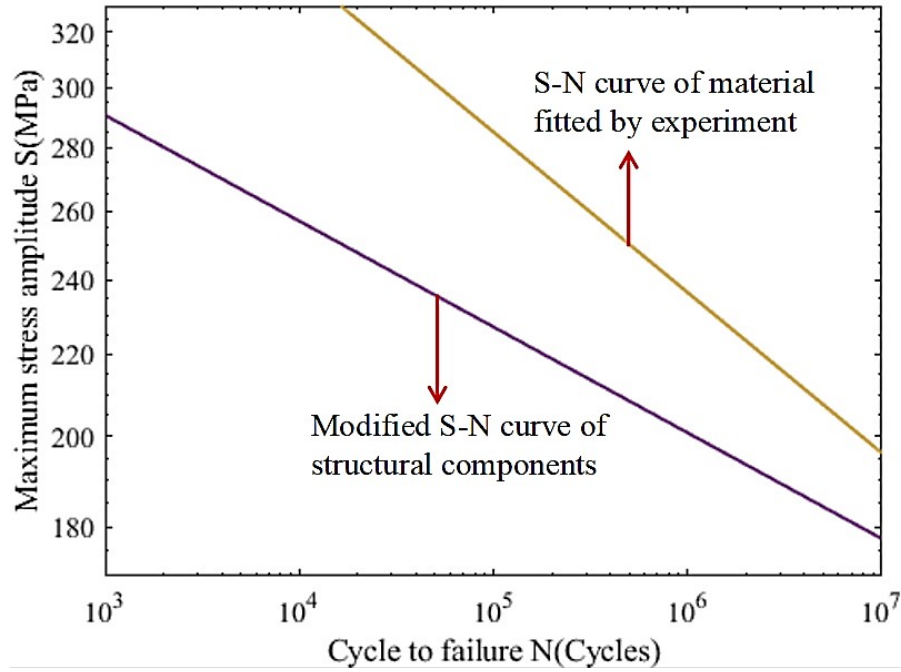
Fig.6. The modified *S-N* curve for fan blade structure.

In order to predict the fatigue life of fan blades, Miner's linear damage accumulation theory was commonly used in the numerical procedure [22]. Damage caused by the fatigue increase in each stress range can been calculated by following Eq. (13):

$$D = \sum_i \frac{n_i}{N_i} \tag{13}$$

where n_i is the number of cycles of load applied within the stress range and N_i represents the failure of the component when its cycle number is N_i. When the cumulative damage (*D*) is equal to one, blade

failure is assumed to occur.

According to the records of the supplier, the fan had four different rotating speeds under the actual operating conditions, which were 1600 rpm, 1800 rpm, 2000 rpm and 2200 rpm respectively. The corresponding number of start-stop cycles per year was shown in Table 4. The finite element analysis results showed that the stress of a blade under a uniform rotation working condition was smaller than the yield stress of the material, and the fatigue was mainly due to the alternating stress caused by the start-stop working mode of the fan.

Table 4

Life prediction of fan blade.

Revolving speed(rpm)	Von Mises stress(MPa)	Number of cycles(n_i)	Fatigue resistances(N_i)
1600	214.12	10519	294188
1800	235.20	1945	55158
2000	258.30	311	9538
2200	282.41	103	1699

The cumulative fatigue damage of the fan after one year of operation was estimated as follows, based on Table 4.

$$D=\sum_{i=4}^{4} \frac{n_i}{N_i} \tag{14}$$

$$D=\left[\frac{10519}{294188}+\frac{1945}{55158}+\frac{311}{9538}+\frac{103}{1699}\right]=0.164 \tag{15}$$

As the total damage of each stress was less than 1.00, the fan blade meets the requirements under the above loading conditions. This means that 17% of the total fatigue life of the year had been consumed.

Since the working condition of the fan was basically the same every year, the total fatigue life of the fan blade was calculated as follows:

$$T = \frac{1}{D} = \frac{1}{0.164} = 6.09 \ years \tag{16}$$

where T was the total fatigue life of the fan blade.

According to the design standard GB/T 13275-91 for high-speed rail centrifugal fan blades, the design life of the fans must be more than 5 years. In this study, the predicted life was 6.09 years, therefore the design requirements for the fatigue life could be met.

4. Fatigue bench test of fan blades

4.1. Test bench construction

A fan fatigue bench was established to validate the simulation results. The test platform and equipment shall include: variable frequency control cabinet, variable frequency speed motor, speed sensor, high speed mercury slip ring, dynamic strain testing system, software system and so on. Fig. 7A and B show the experimental principle and the experimental site, respectively.
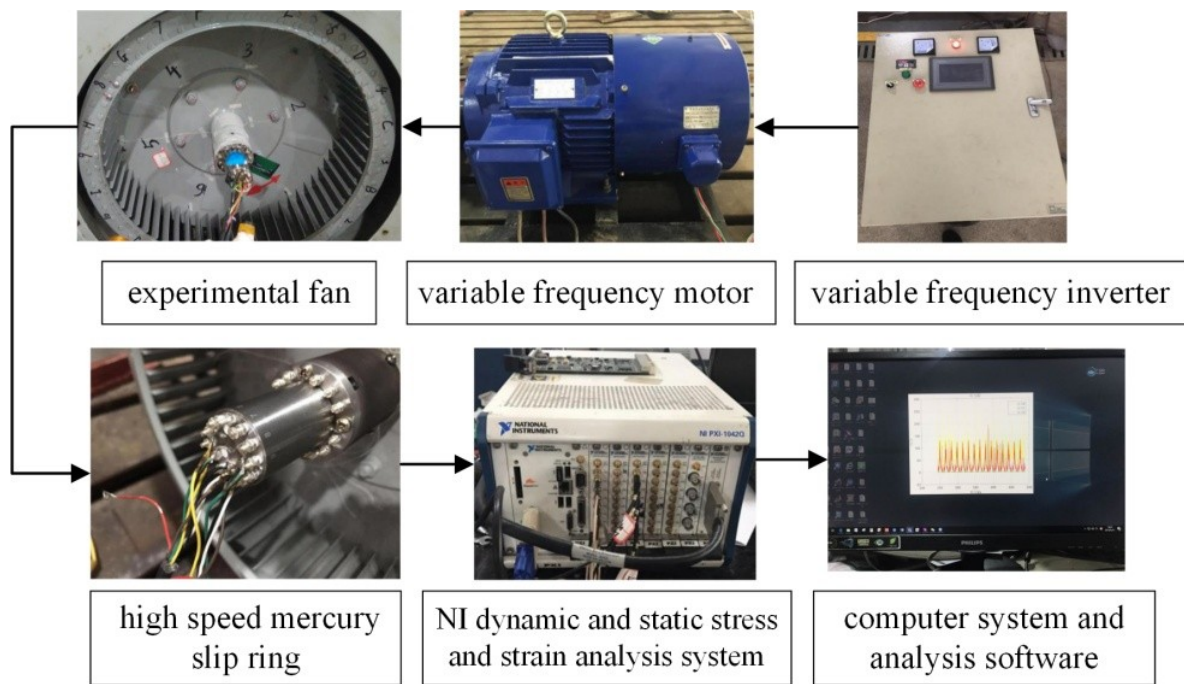
(A)
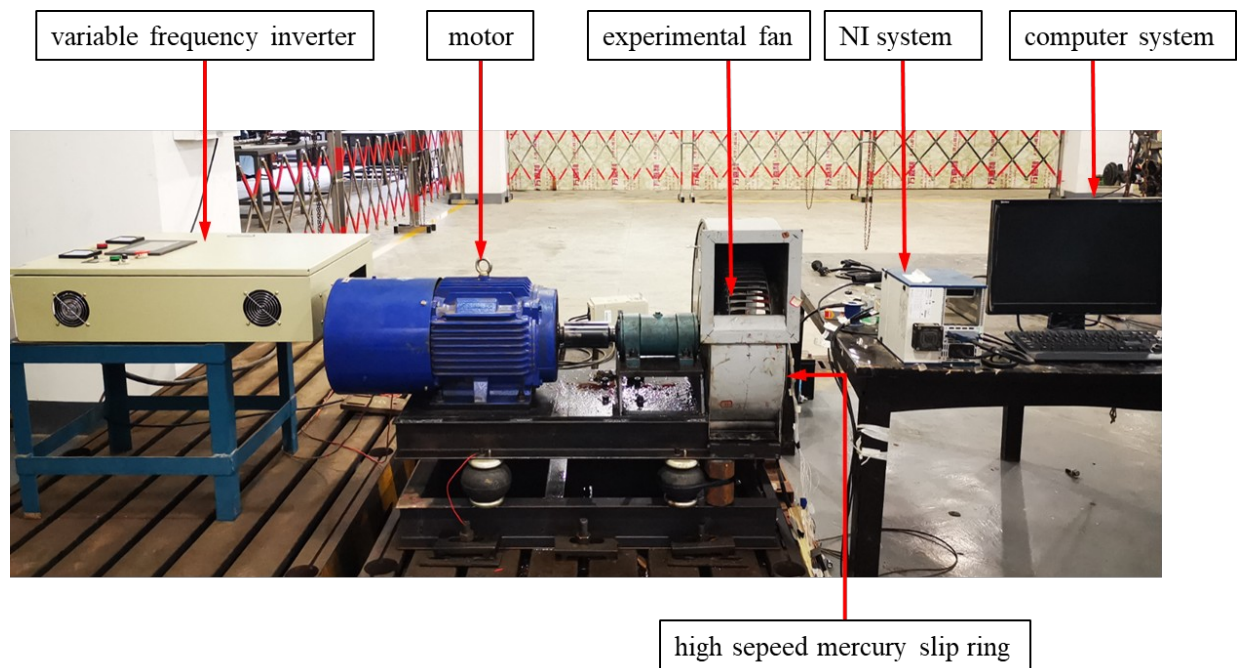
(B)

Fig.7. The fan fatigue test system. (A) The fatigue test strain data acquisition system. (B) The components of the fan blade fatigue test system.

The essence of test was to measure the strain based on the stress and strain values of different measuring points on the structure surface. The real-time stress values could be calculated by a graphical program compilation platform developed by America national instrument company NI. In order to determine the position of the measuring point, the strain should be selected in the position of greater stress or easy to damage. In this paper, the stress state of the impeller structure was calculated by using the finite element method, and partitioned the fan. To ensure the accuracy of the measured data, the root paint of the blade was removed. Finally, six of the blades were selected to stick strain gauge and the strain gauge was pasted on the root of the blade to measure the stress in the X-direction, as shown in Fig. 8.
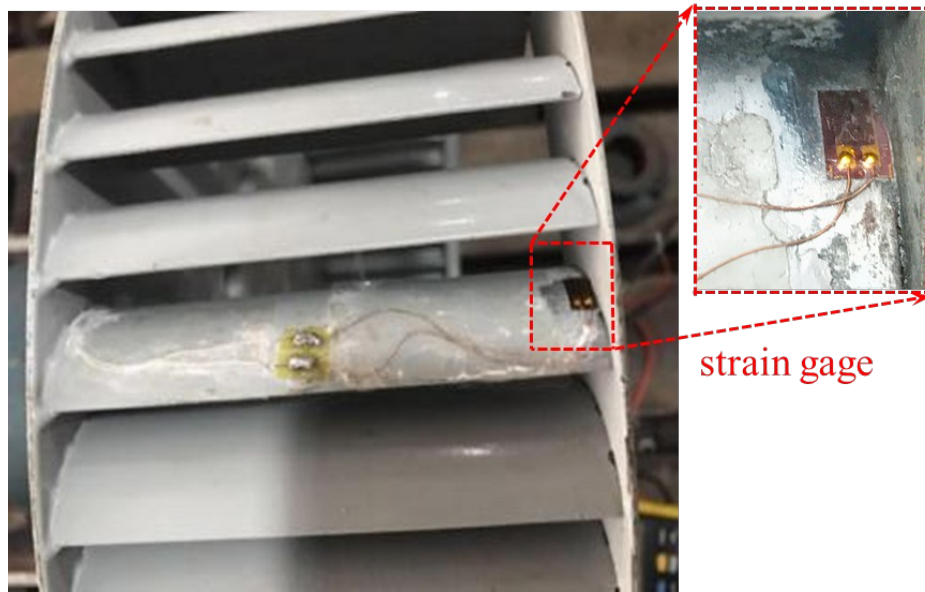

Fig.8. Position of strain gauge paste.

The other end of the high-temperature wire joined up the terminal of the rotor side of the high-speed slip ring. Meanwhile, the terminals of the corresponding stator side were connected to the wire, and attached to the response channel of the NI scxi-1317 junction box in a uniform order. Then,

the junction box was installed into the NI pxi-6224 strain data acquisition card that had been placed in the card slot of NI pxi-1042q chassis. The speed photoelectric sensor was placed on the shaft end of the fan to collect speed signal, which was connected to NI data acquisition card successively. After all the instruments were linked, the initial measurement was calibrated by LabVIEW software.

4.2. Fan blades fatigue test

The fatigue tests were carried out in the form of trapezoidal wave with a loading frequency of 0.04 Hz, as shown in Fig. 9, under normal temperature and atmospheric conditions. Stress ratio (R=0) was conducted in all tests. The stress range measured by the test system was 0~5000 MPa, and the range of rising speed at this frequency was 0~3000 rpm. The actual working condition of the fan was simulated to the maximum extent. In order to ensure that each revolving speed range could be accelerated to the specified speed, the differences of accelerations at different speeds were taken into account.
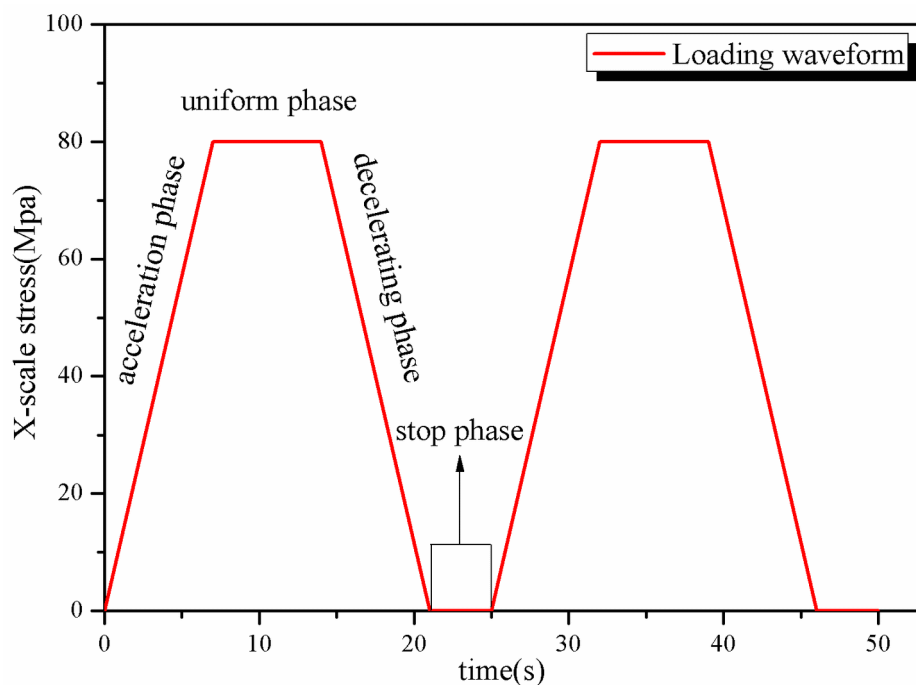

Fig.9. The fatigue load spectra for fan blade

19

Experiments were carried out based on the predicted model, and fatigue life tests were conducted on fan blades under four different levels of constant stress. The starting and stopping test was carried out at 1600 rpm firstly, and then the 1800 rpm, 2000 rpm and 2200 rpm tests were done. There were at least four sample fans were used for each set of the fatigue life test. Then, the cumulative fatigue tests were carried out at four levels of 1600~2200 rpm speed and at least 4 sample fans were used in the fatigue life test. In order to detect the onset of fatigue cracking, the response of each critical section and dangerous part was monitored and observed at different test time during the fatigue test. The fatigue crack propagation was observed and recorded. A crack with a length of 6mm appears on the surface near the root of the connecting end of blade and impeller, indicating impeller failure, as shown in Fig. 11.

4.3. Test data processing

In this study, the data were copied and analyzed in time segments, and the stress-strain diagram was drawn by MATLAB programming, which was convenient for intuitive observation of data changes in the test process. By means of rain-flow counting method [44], all load cycles were extracted from the load history and the number of load cycles was statistically computed.
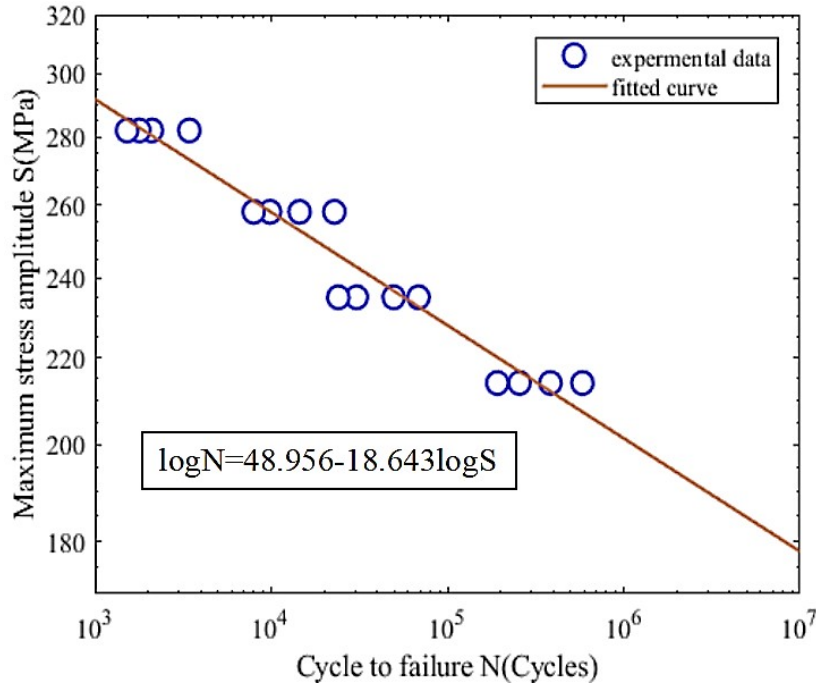
Fig. 10. The *S-N* curve for fan blades.

From Eq. (1), according to the experimental data in Fig. 10, the *S-N* curve of fan blades at different stress levels when the stress ratio was 0 could be determined as

$$\log N = 48.956 - 18.643 \log S \tag{17}$$

Eq. (17) was drawn in Fig.10 which showed a relatively good correlation with the experimental date and the predicted curve. Therefore, it was considered that the *S-N* curve of Eq. (1) sufficient and logically describes the physical characteristics and phenomenological quantitative rules of fan blades. What counts was the parameters of the model can be conveniently and easily determined. As shown in Fig. 11 it could be seen that the fatigue failure mode of the measured fan blade could be considered as a feature of fatigue crack initiation and propagation, starting from the edge angle of blade root to the penetration and fracture of blade root.
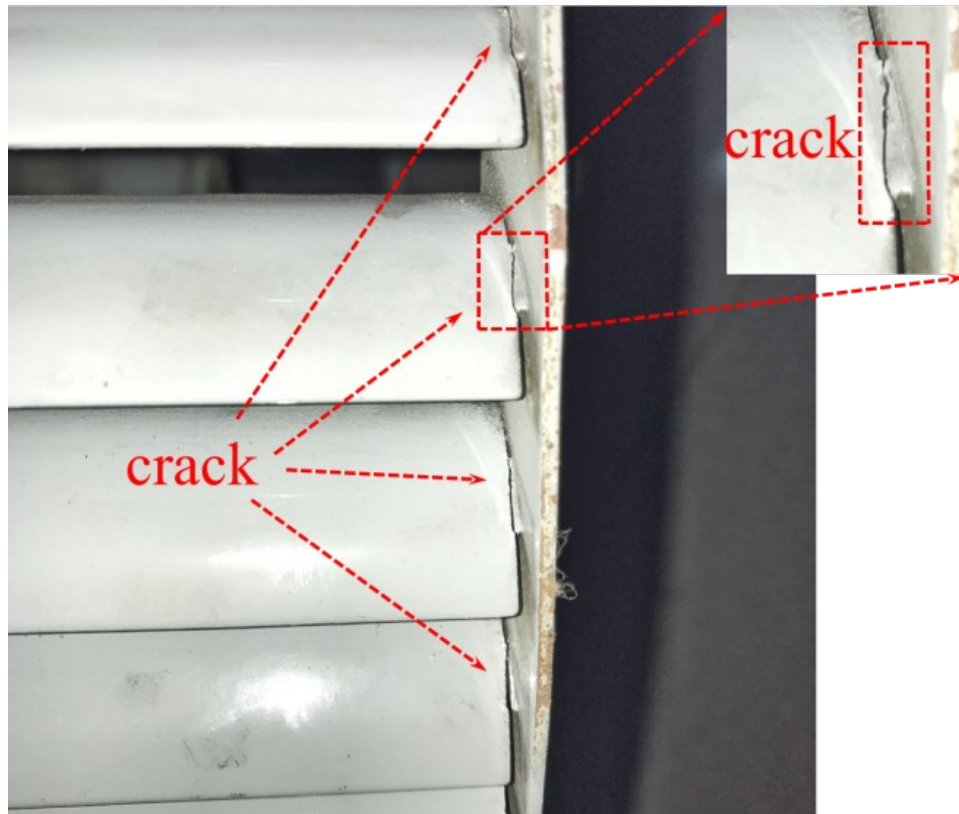
Fig.11. Failure location of blade root area (S_{max} = 214.12 MPa, N = 2.56*10^5 cycles).

(a) Failure picture   (b) Fractography
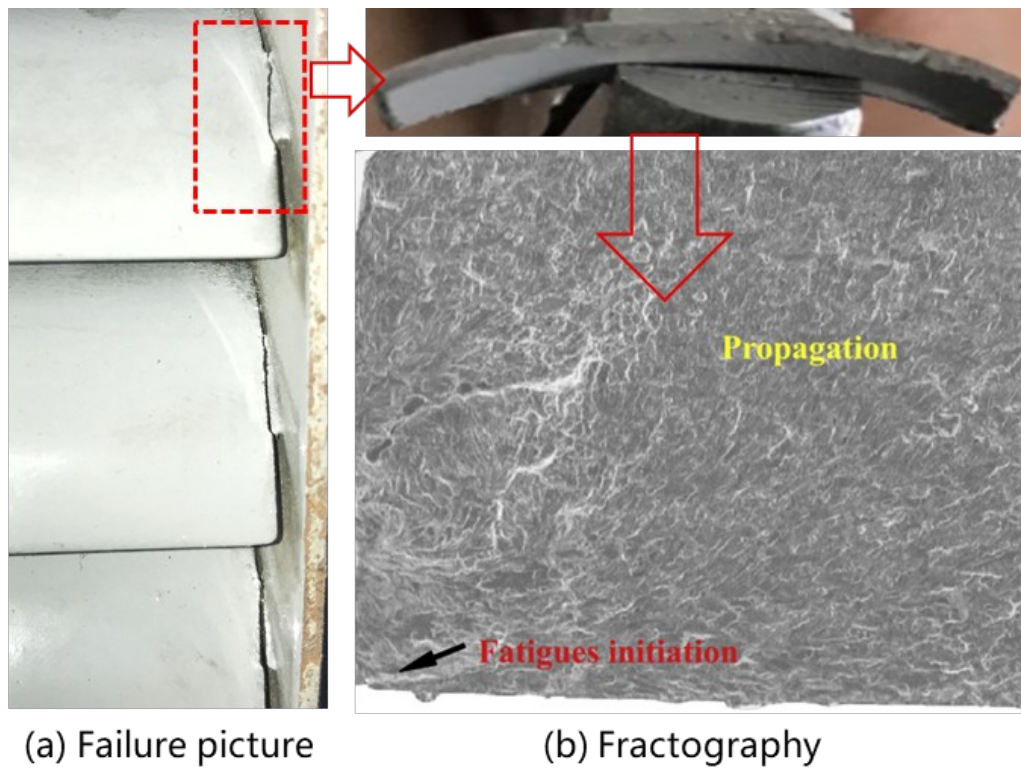
Fig.12. Fractography for blade.

22

From the experimental observation, as shown in Fig. 12(a), it was clearly seen that the fatigue failure modes of the fan blades could be reckoned to be the characteristics of fatigue crack initiation and propagation from the edge of blades root until the blades penetration and rupture. In order to understand the fatigue damage mechanisms of blade roots, scanning electron microscope (SEM) was used to analyze the fracture surfaces of the failed blades, so as to provide direct evidence of crack nucleation and growth in areas that could not be observed visually. Fig. 12(b) showed the obvious fatigue origin and fracture propagation zone during the fatigue process. Obviously, the fatigue origin started out in the edge corner of blade root (consistent with the position predicted by finite element method), and then the fatigue crack propagated radially outward from the origin of fatigue, and finally completely broke the blade root, leading to blade failure. Whereas, from the macro level the blade surface did not seem to be damaged, and the failure mode was the fatigue crack nucleation and growth given rise to the fracture of blade root. As a consequence, it could be concluded that the fatigue failures of root of blade was the primary reasons to cause the failure of fan blade.

Table 5

Fatigue life of four kinds of fans with different rotating speeds under spectral loads.

Revolving speed（rpm)	Experimental fitting (Number of cycles)	Prediction (Number of cycles)	Relative deviation
1600	323665	294188	10.0%
1800	56517	55158	2.5%
2000	9912	9538	3.9%
2200	1888	1699	11.1%

Table 6

Cumulative fatigue test of fans.

Number of test fans	Experimental life(years)	Mean life(years)	Prediction life(years)	Relative deviation
4	6.18,6.78,6.91,7.12	6.75	6.09	10.8%

4.4. Comparison between predictions and experiments

The stress measured at different speeds in the above experiments was substituted into the matlab fitting program, and the fitting curve was expressed as Eq.(17) based on Eq.(1). The fatigue life of fan blades under different working conditions was calculated (Fig. 10) as listed in Table 5. The number of cycles measured in the above test was substituted into Eq.(14).The cumulative fatigue life was shown in Table 6.The predicted fatigue life was compared with the experimental data, the relative errors between the predicted results and the experimental data were shown in Table 5 and Table 6. It could be seen that the relative deviations between theoretical prediction and experimental results with revolving speeds of 1600 rpm, 1800 rpm, 2000 rpm and 2200 rpm were about 10.0%, 2.5%, 3.9% and 11.1% respectively, and the error between the cumulative fatigue life test and Miner's theoretical calculation was 10.8% with acceptable dispersion. Therefore, the improved method based on the concept of the nominal stress could effectively predict of the fatigue lifetime of complex fan blades.

In addition, it is well known that the fatigue life outcomes tend to be much dispersed [45]. Therefore, in general, the general rule and analysis results of high reliability can be obtained through repeated large sample experiments. Under the circumstances, resources often limit the number of experiments. When more specimens and more stress levels are noticed for the fatigue tests, more accurate fatigue properties would be determined which makes results more accurate.

It was clear that through modified method (6) and (7), the fatigue lifetime of the fan blades subjected to different rotating speed conditions could conveniently and easily be predicted by the

minimum data set of a small number of experimental fans without any additional experimental studies. In short, the fatigue life of fan blades under different working conditions could be predicted only by obtaining the maximum stress of fan blades' model and the *S-N* curve of materials. The correlation between prediction results and actual experimental results was relatively good.

5. Conclusions

A method of predicting the fatigue life based on the *S-N* curve and mean stress was proposed in this study, and a special application dedicated to the ventilation cooling system of the high-speed-train was investigated. The effectiveness of the prediction model was confirmed through a comparison with the fatigue bench test system. The primary conclusions were summarized as follows:

(1) The maximum stress of the fan was calculated by using the finite element method, and the stress concentration was located at the root of the blade.

(2) The fatigue prediction model was based on mean stress and also took several specificities of the fan structure (SCF, surface quality coefficient…) into consideration. By means of the *S-N* curve of the material, the fan's life was predicted by using this new prediction model according to equivalent life curve and cumulative damage criterion.

(3) The fan fatigue test system with adjustable frequency was built. Experimental results showed that the method was successful, in which reasonable correlation was achieved between predictions and actual experiments. According to the fatigue life prediction model, reducing the stress concentration is an effective way to increase the fatigue life of a component. Hence, to improve the service life of the fans, the method which can help to reduce stress concentration

such as making an arc or adding a stress groove at the blade root was recommended.

Reference

1. Adam N, Macha E. Spectral method in multiaxial random fatigue. Lecture Notes in Applied & Computational Mechanics. 2005;33.

2. Xu L, Wang Q, Zhou M. Micro-crack Initiation and Propagation in a High Strength Aluminum Alloy during Very High Cycle Fatigue. Materials science Engineering A. 2018;715(FEB.7):404-13.

3. Susmel L. The modified wöhler curve method and cracking behaviour of metallic materials under fatigue loading. Aircr Eng. 2009:189-209.

4. Agoda T, Macha E, Pawliczek R. The influence of the mean stress on fatigue life of 10HNAP steel under random loading. Int J Fatigue. 2001;23(4):283-91.

5. Kang G, Liu Y. Uniaxial ratchetting and low-cycle fatigue failure of the steel with cyclic stabilizing or softening feature. Mater Sci Eng, A. 2008;472(1-2):258-68.

6. Poursaeidi E, Babaei A, Behrouzshad F, et al. Failure analysis of an axial compressor first row rotating blades. Eng Fail Anal. 2013;28:25-33.

7. Poursaeidi E, Bakhtiari H. Fatigue crack growth simulation in a first stage of compressor blade. Eng Fail Anal. 2014;45:314-25.

8. Urban M. Analysis of the fatigue life of riveted sheet metal helicopter airframe joints. Int J Fatigue. 2003;25(9-11):1013-26.

9. Kim J, Yoon JC, Kang BS. Finite element analysis and modeling of structure with bolted joints. Applied Mathematical Modelling. 2007;31(5):895-911.

10. Oskouei R, Keikhosravy M, Soutis C. A finite element stress analysis of aircraft bolted joints loaded in tension. J Aeronaut Sci. 2010;114(1155):315-20.

11. Abu AO, Eshati S, Laskaridis P, et al. Aero-engine turbine blade life assessment using the Neu/Sehitoglu damage model. Int J Fatigue. 2014;61:160-9.

12. Peč M, Zapletal J, Šebek F, et al. Low-cycle fatigue, fractography and life assessment of EN AW 2024-T351 under various loadings. Experimental Techniques. 2019;43(1):41-56.

13. Tulsidas D, Shantharaja M, Bharath VG. Life estimation of a steam turbine blade using low cycle fatigue analysis. Procedia Mater Sci. 2014;5:2392-401.

14. Dungey C, Bowen P. The effect of combined cycle fatigue upon the fatigue performance of TI–6AL–4V fan blade material. J Mater Process Technol. 2004;153-154:374-9.

15. Hou N, Wen Z, Yu Q, et al. Application of a combined high and low cycle fatigue life model on life prediction of SC blade. Int J Fatigue. 2009;31(4):616-9.

16. Vargas JA, Wilches JE, Gómez HA, et al. Analysis of catastrophic failure of axial fan blades exposed to high relative humidity and saline environment. Eng Fail Anal. 2015;54:74-89.

17. Schweizer C, Seifert T, Nieweg B, et al. Mechanisms and modelling of fatigue crack growth under combined low and high cycle fatigue loading. Int J Fatigue. 2011;33(2):194-202.

18. Stanzl-Tschegg SE, Meischel M, Arcari A, et al. Combined cycle fatigue of 7075 aluminum alloy – Fracture surface characterization and short crack propagation. Int J Fatigue. 2016;91:352-62.

19. Zheng X, Engler-Pinto CC, Su X, et al. Modeling of fatigue damage under superimposed high-cycle and low-cycle fatigue loading for a cast aluminum alloy. Mater Sci Eng, A. 2013;560:792-801.

20. Nelson DV, Fuchs HO. Predictions of cumulative fatigue damage using condensed load histories. Advances in Engineering. 1997;6:163-87.

21. Shahani AR, Mohammadi S. Damage tolerance and classic fatigue life prediction of a helicopter main rotor blade. Meccanica. 2015;51(8):1869-86.

22. M.A. M. Cumulative damage in fatigue. J Appl Mech. 1945;12(3):159-64.

23. Zhu S-P, Yue P, Yu Z-Y, et al. A combined high and low cycle fatigue model for life prediction of turbine blades. Materials. 2017;10(7):698.

24. Bernstein HL, Grant TS, McClung RC, et al. Prediction of thermal-mechanical fatigue life for gas turbine blades in electric power generation. In: Sehitoglu H, editor. Thermomechanical Fatigue Behavior of Materials. West Conshohocken, PA: ASTM International; 1993. p. 212-38.

25. Vardar N, Ekerim A. Failure analysis of gas turbine blades in a thermal power plant. Engineering Failure Analysis. 2007;14(4):743-9.

26. Shi L, Wei D-s, Wang Y-r, et al. An investigation of fretting fatigue in a circular arc dovetail assembly. Int J Fatigue. 2016;82:226-37.

27. Maktouf W, Ammar K, Ben Naceur I, et al. Multiaxial high-cycle fatigue criteria and life prediction: Application to gas turbine blade. Int J Fatigue. 2016;92:25-35.

28. Mangardich D, Abrari F, Fawaz Z. Modeling crack growth of an aircraft engine high pressure compressor blade under combined HCF and LCF loading. Eng Fract Mech. 2019;214:474-86.

29. Cano S, Rodriguez JA, Rodriguez JM, et al. Detection of damage in steam turbine blades caused by low cycle and strain cycling fatigue. Eng Fail Anal. 2019;97:579-88.

30. Heege A, Betran J, Radovcic Y. Fatigue load computation of wind turbine gearboxes by coupled finite element, multi-body system and aerodynamic analysis. Wind Energy. 2010;10(5):395-413.

31. Chen X. Experimental observation of fatigue degradation in a composite wind turbine blade. Compos Struct. 2019;212:547–51.

32. Grbovic A, Kastratovic G, Sedmak A, et al. Fatigue crack paths in light aircraft wing spars. Int J Fatigue. 2019;123:96-104.

33. Coppotelli G. Experimental identification of the structural properties of an AB 204: Helicopter blade and finite element model validation. Experimental Techniques. 2009;33(5):25-34.

34. Ravi Chandran KS, Jha SK. Duality of the S–N fatigue curve caused by competing failure modes in a titanium alloy and the role of Poisson defect statistics. Acta Materialia. 2005;53(7):1867-81.

35. Xu F, Li CR, Jiang TM, et al. Fatigue life prediction for PBGA under random vibration using updated finite element models. Experimental Techniques. 2016;40(5):1421-35.

36. Kreethi R, Sivateja C, Mondal AK, et al. Ratcheting life prediction of quenched–tempered 42CrMo4 steel. J Mater Sci. 2019;54(17):11703-12.

37. Kubair DV, Bhanu-Chandar B. Stress concentration factor due to a circular hole in functionally graded panels under uniaxial tension. Int J Mech Sci. 2008;50(4):732-42.

38. Louhghalam A, Igusa T, Park C, et al. Analysis of stress concentrations in plates with rectangular openings by a combined conformal mapping – Finite element approach. Int J Solids Struct. 2011;48(13):1991-2004.

39. Carpinteri A. A fractal analysis of size effect on fatigue crack growth. Int J Fatigue. 2004;26(2):125-33.

40. J.J. Xiong, Shenoi RA. Fatigue and fracture reliability engineering: London: Springer; 2011.

41. Goodman J. Mechanics applied to engineering: London: Longmans, Green & Company; 1919.

42. Tasdighi E, Nobakhti H, Soltani N. Application of small punch test in predicting the axial fatigue life of 304 stainless steel sheets. Experimental Techniques. 2016;40(4):1349-57.

43. Niesłony A, Böhm M. Mean stress effect correction using constant stress ratio S–N curves. Int J Fatigue. 2013;52:49-56.

44. Musallam M, Johnson CM. An efficient implementation of the rainflow counting algorithm for life consumption estimation. IEEE Trans Reliab. 2012;61(4):978-86.

45 Akhil V, Farshid S. An anisotropic damage model for tensile fatigue. Fatigue Fract Eng Mater Struct, 2018;1–14.